



This is a repository copy of *Characterization of multi-layered tissue engineered human alveolar bone and gingival mucosa*.

White Rose Research Online URL for this paper:  
<http://eprints.whiterose.ac.uk/123618/>

Version: Accepted Version

---

**Article:**

Almela, T., Al-Sahaf, S., Bolt, R. et al. (2 more authors) (2018) Characterization of multi-layered tissue engineered human alveolar bone and gingival mucosa. *Tissue Engineering Part C: Methods*. ISSN 1937-3384

<https://doi.org/10.1089/ten.TEC.2017.0370>

---

Final publication is available from Mary Ann Liebert, Inc., publishers  
<http://dx.doi.org/10.1089/ten.TEC.2017.0370>

**Reuse**

Items deposited in White Rose Research Online are protected by copyright, with all rights reserved unless indicated otherwise. They may be downloaded and/or printed for private study, or other acts as permitted by national copyright laws. The publisher or other rights holders may allow further reproduction and re-use of the full text version. This is indicated by the licence information on the White Rose Research Online record for the item.

**Takedown**

If you consider content in White Rose Research Online to be in breach of UK law, please notify us by emailing [eprints@whiterose.ac.uk](mailto:eprints@whiterose.ac.uk) including the URL of the record and the reason for the withdrawal request.



[eprints@whiterose.ac.uk](mailto:eprints@whiterose.ac.uk)  
<https://eprints.whiterose.ac.uk/>



This is an author produced version of *Characterization of Multi-layered Tissue Engineered Human Alveolar Bone and Gingival Mucosa*.

White Rose Research Online URL for this paper:  
<http://eprints.whiterose.ac.uk/123618/>

---

**Article:**

almela, T, Al-Sahaf, S, bolt, R et al. (2 more authors) (2017) Characterization of Multi-layered Tissue Engineered Human Alveolar Bone and Gingival Mucosa. Tissue Engineering, Part C, Methods. ISSN 1937-3384 (In Press)

<https://doi.org/10.1089/ten.TEC.2017.0370>

---

# Tissue Engineering

Tissue Engineering Manuscript Central: <http://mc.manuscriptcentral.com/ten>

## Characterization of Multi-layered Tissue Engineered Human Alveolar Bone and Gingival Mucosa

Journal:	<i>Tissue Engineering</i>
Manuscript ID	Draft
Manuscript Type:	Methods Article - Part C
Date Submitted by the Author:	n/a
Complete List of Authors:	Almela, Thafar; University of Sheffield Faculty of Medicine Dentistry and Health, The School of Clinical Dentistry, Academic Unit of Oral & Maxillofacial Medicine & Surgery Alsahaf, Sarmad; University of Sheffield Faculty of Medicine Dentistry and Health, The School of Clinical Dentistry, Academic Unit of Oral & Maxillofacial Medicine & Surgery Bolt, Robert; University of Sheffield Faculty of Medicine Dentistry and Health, The School of Clinical Dentistry, Academic Unit of Oral & Maxillofacial Medicine & Surgery Brook, Ian; University of Sheffield Faculty of Medicine Dentistry and Health, The School of Clinical Dentistry, Academic Unit of Oral & Maxillofacial Medicine & Surgery Moharamzadeh, K. ; University of Sheffield Faculty of Medicine Dentistry and Health, The School of Clinical Dentistry, Academic Unit of Restorative Dentistry
Keyword:	Bone < Applications in Tissue Engineering (DO NOT select this phrase; it is a header ONLY), 3-D Cell Culture < Enabling Technologies in Tissue Engineering (DO NOT select this phrase; it is a header ONLY), Composite Tissues < Applications in Tissue Engineering (DO NOT select this phrase; it is a header ONLY)
Manuscript Keywords (Search Terms):	Bone engineering, oral mucosa engineering, alveolar bone mucosal model, composite tissue engineering
Abstract:	Advances in tissue engineering have permitted assembly of multi-layered composite tissue constructs for potential applications in the treatment of combined hard and soft tissue defects and as an alternative in vitro test model to animal experimental systems. The aim of this study was to develop and characterize a novel three-dimensional combined human alveolar bone and gingival mucosal model based on primary cells isolated from the oral tissues. Bone component of the model was engineered by seeding primary human alveolar osteoblasts (HAOBs) into a hydroxyapatite/tricalcium phosphate (HA/TCP) scaffold and culturing in a spinner bioreactor. The engineered bone was then laminated, using an adhesive tissue sealant, with tissue engineered gingival mucosa consisting of air/liquid interface-cultured normal human gingival keratinocytes on oral fibroblast-populated collagen gel scaffold. Histological characterization revealed a structure consisting of established epithelial, connective tissue,

1  
2  
3  
4  
5  
6  
7  
8  
9  
10  
11  
12  
13  
14  
15  
16  
17  
18  
19  
20  
21  
22  
23  
24  
25  
26  
27  
28  
29  
30  
31  
32  
33  
34  
35  
36  
37  
38  
39  
40  
41  
42  
43  
44  
45  
46  
47  
48  
49  
50  
51  
52  
53  
54  
55  
56  
57  
58  
59  
60

	<p>and bone layers closely comparable to normal oral tissue architecture. The mucosal component demonstrated a mature epithelium undergoing terminal differentiation similar to that characteristic of native buccal mucosa, as confirmed using cytokeratin 13 (CK13) and cytokeratin 14 (CK14) immunohistochemistry. Ultrastructural analysis confirmed the presence of desmosomes and hemi-desmosomes in the epithelial layer, a continuous basement membrane and newly synthesized collagen in the connective tissue layer. Quantitative PCR (qPCR) assessment of osteogenesis-related gene expression showed a higher expression of genes encoded Collagen I (COL1) and Osteonectin (ON) as well as Osteocalcin (OC), Osteopontin (OPN), and Alkaline phosphatase (ALP). ELISA quantification of collagen I, ON, and OC confirmed a pattern of secretion which paralleled the model's gene expression profile. We demonstrate here that replicating the anatomical setting between oral mucosa and the underlying alveolar bone is feasible and the developed model showed characteristics similar to those of normal tissue counterparts. This tri-layered model therefore offers great scope as an advanced, and anatomically-representative tissue-engineered alternative to animal models.</p>

SCHOLARONE™  
Manuscripts

**Characterization of Multi-layered Tissue Engineered Human Alveolar Bone and  
Gingival Mucosa**

Thafar Almela\*, Sarmad Al-Sahaf, Robert Bolt, Ian M. Brook, Keyvan Moharamzadeh \*

School of Clinical Dentistry, University of Sheffield, Claremont Crescent, Sheffield, S10  
2TA UK

*\*Corresponding authors:*

[Tkalmela1@sheffield.ac.uk](mailto:Tkalmela1@sheffield.ac.uk)

[K.moharamzadeh@Sheffield.ac.uk](mailto:K.moharamzadeh@Sheffield.ac.uk)

Thafar Almela; BDS, MSc

University of Sheffield, School of Clinical Dentistry, 19 Claremont Crescent, Sheffield  
S10 2TA

Telephone: +44 (0) 7476828728

Email: Tkalmela1@sheffield.ac.uk

Sarmad Al-Sahaf; BDS, MSc

University of Sheffield, School of Clinical Dentistry ,19 Claremont Crescent, Sheffield, S10  
2TA

Telephone: +44 (0)7425059153

Email: sshal-sahaf1@sheffield.ac.uk

Robert Bolt; BDS (Hons), MFDS, MBChB (Hons), MClinRes PhD, MOralSurg.

University of Sheffield, School of Clinical Dentistry 19 Claremont Crescent, Sheffield,  
S10 2TA

Telephone: +44(0)114 2265463

Email: r.bolt@sheffield.ac.uk

Ian M. Brook; BDS MDS FDSRCS(Eng) PhD

The School of Clinical Dentistry, University of Sheffield, 19 Claremont Crescent, Sheffield  
S10 2TA

Telephone: +44(0) 1142717851

Email: i.brook@sheffield.ac.uk

Keyvan Moharamzadeh; BSc, DDS, PhD, FHEA, FDSRCS

The School of Clinical Dentistry, University of Sheffield, 19 Claremont Crescent, Sheffield  
S10 2TA

Telephone: +44(0) 1142717910

Email: K.moharamzadeh@sheffield.ac.uk

The study was performed in School of Clinical Dentistry, University of Sheffield, Claremont  
Crescent, Sheffield, S10 2TA UK.

**Abstract**

Advances in tissue engineering have permitted assembly of multi-layered composite tissue constructs for potential applications in the treatment of combined hard and soft tissue defects and as an alternative in vitro test model to animal experimental systems. The aim of this study was to develop and characterize a novel three-dimensional combined human alveolar bone and gingival mucosal model based on primary cells isolated from the oral tissues. Bone component of the model was engineered by seeding primary human alveolar osteoblasts (HAOBs) into a hydroxyapatite/tricalcium phosphate (HA/TCP) scaffold and culturing in a spinner bioreactor. The engineered bone was then laminated, using an adhesive tissue sealant, with tissue engineered gingival mucosa consisting of air/liquid interface-cultured normal human gingival keratinocytes on oral fibroblast-populated collagen gel scaffold. Histological characterization revealed a structure consisting of established epithelial, connective tissue, and bone layers closely comparable to normal oral tissue architecture. The mucosal component demonstrated a mature epithelium undergoing terminal differentiation similar to that characteristic of native buccal mucosa, as confirmed using cytokeratin 13 (CK13) and cytokeratin 14 (CK14) immunohistochemistry. Ultrastructural analysis confirmed the presence of desmosomes and hemi-desmosomes in the epithelial layer, a continuous basement membrane and newly synthesized collagen in the connective tissue layer. Quantitative PCR (qPCR) assessment of osteogenesis-related gene expression showed a higher expression of genes encoded Collagen I (COL1) and Osteonectin (ON) as well as Osteocalcin (OC), Osteopontin (OPN), and Alkaline phosphatase (ALP). ELISA quantification of collagen I, ON, and OC confirmed a pattern of secretion which paralleled the model's gene expression profile. We demonstrate here that replicating the anatomical setting between oral mucosa and the underlying alveolar bone is feasible and the developed model showed characteristics similar to those of normal tissue counterparts. This tri-layered model therefore offers great scope as an advanced, and anatomically-representative tissue-engineered alternative to animal models.

**Keywords:** Bone engineering, oral mucosa engineering, alveolar bone mucosal model, composite tissue engineering.

## 1. Introduction

The orofacial region is a highly complex anatomical structure, comprising a large number of tissue types within a relatively small area. Restoration of defects following trauma, excision of pathology, and in the correction of developmental deformities, poses a great challenge due to the lack of suitable donor sites for harvesting grafts capable of accurately replicating the missing tissues. Whilst the need for anatomically-accurate grafting materials offers a niche that could be filled using refined tissue engineered constructs, it also imposes a considerable challenge to current composite tissue engineering techniques in order to create and attach the numerous tissue types required to replicate the normal anatomy of this region.<sup>(1)</sup> Despite this challenge, 3D *in vitro* screening systems, based on human cells and tissues, have already attracted significant attention, as they offer more robust and predictive experimental data compared to 2D or animal models.<sup>(2)</sup> Limitations of 2D models include the loss of a natural 3D environment, which is in turn reflected in cell behaviour,<sup>(3)</sup> and additionally the absence of a 3D environment excludes important factors such as hypoxic gradients and drug penetration. Furthermore, animal studies may be misleading due to interspecies molecular and physiological differences.<sup>(4)</sup> Therefore, the short-term need for anatomically-representative 3D models of the oro-facial region is assured. Future development of these models beyond experimental analysis furthermore offers potential to achieve the longer-term goal of establishing tissue engineered grafting materials capable of improving and simplifying the reconstruction of surgical defects in the orofacial region.

Over the last few decades, there has been a substantial amount of innovation and progress in the engineering of various tissues found in the orofacial region, such as cartilage, bone, mucosa, and periodontium.<sup>(5)</sup> This has encouraged researchers to develop more intricately-structured hybrid tissues that differ in the characteristics of their constituent parts, yet comprise a single functional unit. To date, only a few examples of composite tissues have



1  
2  
3 been engineered which replicate the orofacial region. Recent successes include the  
4  
5 engineering of osteochondral components of the temporomandibular joint, which comprises  
6  
7 both articular cartilage and subchondral bone; <sup>(6, 7)</sup> and the engineering of a ligamentous  
8  
9 interface between tooth and alveolar bone to replicate the bone-periodontal ligament  
10  
11 complex.<sup>(8)</sup>  
12  
13

14  
15 Despite these advances, the three key components of the majority of orofacial tissues are that  
16  
17 of bone, fibrous connective tissue and an overlying epithelium. Development of an accurate  
18  
19 alveolar bone-mucosal model therefore represents another important step in the process of  
20  
21 achieving a clinically utilisable tissue engineered orofacial construct. We previously reported  
22  
23 the feasibility of tissue engineering such a model using cancer and immortal cell lines,<sup>(9)</sup>  
24  
25 although acknowledged that patient-sourced primary cells are essential for such a model to be  
26  
27 developed to create a more accurate representation of native tissue.  
28  
29

30  
31 The aim of this study was to develop a novel three-dimensional combined human alveolar  
32  
33 bone and gingival mucosal model based on primary cells isolated from the native human oral  
34  
35 hard and soft tissues and to characterize this model qualitatively and quantitatively to  
36  
37 examine whether it accurately replicates the normal tissues in terms of histology,  
38  
39 ultrastructural appearance, differentiation and phenotype characteristics.  
40  
41  
42  
43  
44  
45  
46  
47  
48  
49  
50  
51  
52  
53  
54  
55  
56  
57  
58  
59  
60

## 2. Materials and Methods

### 2.1. Study design

Gingival biopsies and bone chips were obtained with written, informed consent from patients undergoing elective oral surgery at Charles Clifford Dental Hospital, Sheffield, UK, under appropriate ethical approval from National Research Ethics Services Committee (number 15/LO/0116). The study included simultaneous tissue engineering of oral mucosal model (OMM) and bone model (BM), then combining both to form a composite alveolar bone mucosal model (ABMM) (Figure1). All materials were purchased from Sigma Aldrich, UK unless otherwise stated.

### 2.2. Isolation and cultivation of primary human gingival cells

Normal human oral keratinocytes (NHOKs) and normal human oral fibroblasts (NHOFs) were isolated from gingival biopsies as previously described with some modifications.<sup>(10)</sup> Briefly, the gingival tissues were collected and kept for 4-5 hours at 4°C in transport medium consisting of serum free Dulbecco's Modified Eagles Medium (DMEM)-GlutaMAX™ (Gibco, USA) supplemented with 100 IU:100 mg ml<sup>-1</sup> penicillin-streptomycin (P/S) and 625 ng ml<sup>-1</sup> fungizone. NHOKs were then enzymatically isolated from the biopsies by incubating the tissue in 0.25% trypsin-EDTA for 14-16 hours at 4°C. The epithelial layer was then scraped, cut into small pieces, and plated in 25 cm<sup>2</sup> tissue culture flask at a density of  $1.5 \times 10^6$  with an equal number of i3T3 feeder layer fibroblasts. The keratinocytes were then cultured in a humidified atmosphere of 5 % CO<sub>2</sub> /95 % air at 37 °C in Green's medium.<sup>(11)</sup>

NHOFs were isolated from the connective tissue layer by incubating in 0.05% (w/v) collagenase type I (Gibco, USA) in DMEM-GlutaMAX™ containing 10% Fetal bovine serum (FBS) at 37 °C for 4 hours. The digested tissue was then centrifuged at 200 g for 5 minutes, and the resultant pellet re-suspended in complete DMEM (CDMEM; DMEM-

GlutaMAX™ supplemented with 10% FBS, 625 ng/mL fungizone, and 100 IU:100 mg ml<sup>-1</sup> P/S).

Both NHOKs and NHOFs were fed three times a week until confluency and then used at passage 2.

**2.3. Isolation and cultivation of primary human alveolar osteoblasts**

Primary human alveolar osteoblasts (HAOBs) were isolated from bone chips collected in a sterile bone trap during preparation of dental implant sites.<sup>(12, 13)</sup> After collection in transport medium, the osseous tissues were extensively rinsed in phosphate buffered saline (PBS) and vortexed to remove blood components. Bone fragments were cultured as explants in 75 cm<sup>2</sup> flask in CDMEM supplemented with 50 µg/ml L-ascorbic acid 2-phosphate (L-AA) at 37°C in a humidified atmosphere of 95% air, 5% CO<sub>2</sub>. The culture was left undisturbed for 7 days, after which the medium was replaced 2-3 times/week until the culture attained confluency, whereby cells were detached by trypsin/EDTA (0.25%), sub cultured, and used in the 3<sup>nd</sup> passage.

**2.4. Engineering the oral mucosal models (OMMs)**

Collagen-based OMM was constructed according to the technique described by Dongari-Bagtzoglou and Kashleva.<sup>(14)</sup> A solution of 10 × DMEM 13.8 mg ml<sup>-1</sup>, FBS 8.5% (v/v), L-glutamine 2 mM, reconstitution buffer (22 mg ml<sup>-1</sup> sodium bicarbonate and 20 mM HEPES), and 5 mg ml<sup>-1</sup> rat-tail type I collagen (R & D system) was prepared on ice and neutralized by 1M sodium hydroxide to pH=7.4.

Finally, a cell suspension of NHOFs in CDMEM at a concentration of 2×10<sup>5</sup> cells per model was added to the solution. The resultant fibroblast-containing collagen was transferred into tissue culture inserts (0.4 µm pore size, 30 mm diameter, Millipore) and incubated at 37°C for 2 hours until solidified. 1.5 ml CDMEM was then added inside and outside the insert.

After 3 days,  $1 \times 10^6$  NHOK cells (per model) suspended in 50  $\mu$ l Green's medium were seeded on the gel surface and allowed to adhere for 3 hours. 2 ml Green's medium was then gently added into the insert and incubated at 37 °C, 5% CO<sub>2</sub> for 4 days. When epithelial cells reached confluency, the culture was raised to air/liquid interface and fed every other day for 10 days.

## 2.5. Engineering the bone models (BMs)

10 sterile ceramic discs (2mm  $\times$  10mm) of Hydroxyapatite/Tricalcium phosphate (HA/TCP) (60%/40%) (Ceramisis LTD, UK) with total porosity of 78.9 % were used as a scaffold. The discs were placed in 24- well plates and pre-wetted with CDMEM 24 hours before cell seeding.  $2 \times 10^6$  HOBs cells suspended in 15  $\mu$ l CDMEM /L-AA were then added dropwise to each scaffold. The cells were allowed to adhere for 2 hours, and then BMs completely covered with 2 ml CDMEM /L-AA and incubated overnight. After 24 hours, BMs were suspended in a spinner bioreactor (Branstead Stem, UK) and spun at a rate of 30 rpm. The medium was changed every 2 days for 17 days.

## 2.6. Cell viability assessment using PrestoBlue (PB) live assay

The assessment of cell viability within BMs and OMMs was performed using the PB assay (Invitrogen, USA) at day 17 before the combination of the two constructs. BMs and OMMs were separately placed in a 12- well tissue culture plate, washed with PBS, and then a mixture of 900  $\mu$ l of CDMEM and 100  $\mu$ l of PB reagent was added to each well. Three acellular discs and collagen gel were included as negative controls for BMs and OMMs, respectively. After 3 hours incubation at 37°C, the fluorescence values (excitation/emission: 560/590 nm) of 200  $\mu$ l aliquot were measured in triplicates using spectrophotometric plate reader (Infinite® M200, TECAN, USA). For calculation, the average fluorescence values of

the medium containing the scaffolds without cells were subtracted from the averaged sample readings.

**2.7. Engineering the composite alveolar bone mucosal models (ABMMs)**

ABMMs were constructed as previously described.<sup>(9)</sup> At day 17, BM and OMM models were combined using a biocompatible fibrin-based adhesive sealant (ARTISS, Baxter, UK). In brief, BMs were retrieved and placed on a sterile culture plate containing 10 ml CDMEM. The fibrin adhesive was prepared in a pre-filled syringe according to manufacturer's instructions, and a thin layer of the mixed fibrinogen-thrombin sealer applied to the non-epithelial side of an OMM. The OMM was then immediately attached to the surface of a BM and held in the desired position with gentle compression for a minimum of 60 seconds to ensure the adhesive material had completely set, and that both models were firmly adhered to each other. The ABMMs were then further cultured for 5 days, after which the analyses were performed.

**2.8. Histological examination of ABMM**

ABMMs were fixed in 4% paraformaldehyde (PFA) for 24 hours and embedded in 2-hydroxyethyl methacrylate resin (Technovit 7100, Heraeus Kulzer) according to manufacturer's instructions. Briefly, samples were dehydrated in graded ethanol series 75%, 95%, 100% for at least 2 hours, then pre-infiltrated with equal parts of basic solution and 100% ethanol overnight on a rotating mixer. Infiltration was performed with infiltration medium consisting of 100 ml basic solution and 1 g Hardener1. Finally, samples were polymerized in suitable molds with premixed 15 ml infiltration medium and 1 ml Hardener-2. Polymerisation was completed over the period of 2 hours at room temperature.

For routine haematoxylin and eosin (H&E) staining (Leica Microsystems), the ground block was first sectioned into 100-150  $\mu\text{m}$  thickness with a cutting machine (IsoMet<sup>®</sup> 1000 precision saw, Buehler UK Ltd, UK). The section was then adhered to a glass slide using cyanoacrylate adhesive (Loctite<sup>®</sup> glass bond UV curing, UK). The thickness was then further reduced to 30-35  $\mu\text{m}$  by grinding the sections with silicon carbide papers of P800 and P1200 roughness in a grinder-polisher machine (Buehler<sup>™</sup> Metaserv, UK).

## 2.9. Histological, Immunofluorescent (IF), and Transmission Electron Microscopy (TEM) Examinations of OMMs.

OMMs were processed for histological, IF, and TEM examination at the end of culture period. Frozen sections were prepared as previously described.<sup>(15)</sup> OMM were fixed with 4% PFA for 24 hours, followed by an overnight incubation in 18% sucrose in PBS. The samples were frozen in OCT Compound (Thermofisher) and sectioned to 14  $\mu\text{m}$ , and sections were then either stained with H&E for examination under inverted microscope (Olympus, Japan), or were subjected to IF staining.

For IF staining, the sections were washed with PBS for 5 minutes, permeabilized with 0.2 % Triton x-100 for 5 minutes, and then blocked with 1% bovine serum albumin (BSA) in 0.1 % PBS-Tween for 1 hour. The sections were then incubated overnight at 4 °C with conjugated anti-Cytokeratin 13 (Abcam, UK, ab198584) and anti-Cytokeratin 14 (Abcam, UK, ab192055) antibodies at a working dilution of 1:100. After washing, slides were mounted using DAPI-containing mounting medium (Thermofisher, UK) and viewed using IF microscopy (Zeiss Ltd, Germany). Normal oral mucosa (NOM) was used as a positive control, while negative control was OMM stained with IgG isotype (1:100) (ebioscience, UK), followed by goat anti rabbit secondary antibodies (1:200) (Abcam, UK, ab150083).

For TEM analysis, 4mm sections of OMM were fixed in 3% glutaraldehyde in 0.1 M sodium cacodylate buffer for 2 hours at 4°C, and post fixed in 1% osmium tetroxide for 2 hours. Tissue was dehydrated with 70%, 95%, and 100% ethanol and then embedded in resin. Samples were left for 48 hours in the oven at 60 °C, and thereafter examined using a transmission electron microscope (FEI tecnai 12 Bio-twin, 120Kv TEM).

**2.10. Quantitative polymerase chain reaction (qPCR) examination**

For gene expression analysis, ABMMs were snap frozen, grinded, and digested with lysis buffer. RNA was isolated using isolate II RNA Mini Kit (BioLine, UK) according to manufacturer's instructions. 500 ng total RNA was reverse transcribed using a High-Capacity RNA to Complementary DNA (cDNA) kit (Life Technologies, UK).

0.5 µl cDNA was amplified using 5 µl TaqMan gene expression master mix, 3.5 µl nuclease free water and 0.5 µl TaqMan gene probes (Applied Biosystems). Genes encoding the following markers were then interrogated; ALP, Osteopontin (OP), Osteonectin (ON), Osteocalcin (OC), Collagen I (COL1), Ki 67, Cytokeratin 10 (CK10), and Cytokeratin 13 (CK13). B-2-Microglobulin was used as a reference control gene (All Applied biosystem, UK).

Cycling conditions were holding at 95°C for 10 minutes, then 95°C for 10 seconds, followed by 60 °C for 45 seconds and the cycle was repeated 40 times (QIAGEN, Germany). The threshold cycle (Ct) was normalized against the reference gene ( $\Delta$  Ct) and the expression relative to it was calculated.

**2.11. Enzyme-linked immunosorbent assay (ELISA)**

Commercially available ELISA kits for COL1, ON (R&D systems, UK), and OC (Abcam, UK) were used according to manufacturer's instructions in order to quantify these proteins in ABMM after 24 hours incubation in serum free tissue culture conditioned medium. The



solutions were read at absorbance 450 nm using a microplate reader (Infinite® M200, TECAN, USA).

### 2.12. Statistics

All data were presented in terms of mean  $\pm$  SD of three independent experiments performed in triplicate. One-way ANOVA complemented by Tukey's multiple comparisons test was performed using GraphPad Prism v7.0 (GraphPad Software, La Jolla, CA), and differences were considered significant when  $p < 0.05$ .

## 3. Results

### 3.1. Viability assay

Cell viability testing using the PB assay revealed that HAOBs within the bone model as well as NHOFs and NHOKs in the OMM remained vital throughout the experiment (Figure 2).

### 3.2. Histological assessment of ABMM

Histological observation revealed that the ABMM had a structure consisting of epithelial, connective tissue and bony layers which were comparable to the histological architecture of the soft and hard tissues of the oral cavity (Figure 3A). The model's surface displayed a continuous stratified epithelial layer, and a connective tissue layer densely populated with viable fibroblasts (Figure 3B). The hard-soft tissue interface showed a thin band of cell-infiltrated sealant adhering both layers (Figure 3C). Viable cells evenly populated the scaffold porosities with a secreted matrix partially or completely filling the pores of the scaffold (Figure 3D).

### 3.3. OMM assessments

Histologically, the OMM showed a proliferating basal layer and well-differentiated stratified squamous oral epithelium of 12-14 NHOKs thickness, which mimicked that of NOM (Figure 4). The epithelium consisted of four distinct layers that included equivalents to basal, spinous, intermediate, and superficial cells, respectively. The uppermost aspect of the superficial layer



had cells of a flattened appearance, while cells in the basal layer remained rounded. Glycogen granules were occasionally observed in the intermediate layer. NHOFs were found dispersed homogeneously in the connective tissue.

Figure 5 shows the keratin expression of NOM and OMM, as assessed by immunofluorescent staining for CK13 and CK14. The suprabasal cells of the OMM strongly expressed CK13, consistent with the staining of intermediate and superficial cells in para-keratinized stratified epithelium.<sup>(16)</sup> CK14 was expressed throughout the entire epithelium.

Ultrastructural analysis of the OMM demonstrated the presence of numerous desmosomes between adjacent epithelial cells (Figure 6A). A continuous and intact basement membrane was formed, anchoring the epithelium firmly to the connective tissue by means of hemidesmosomal attachments (Figure 6B). In the sup-epithelial layer, a high amount of newly synthesized collagen was observed (Figure 6C).

**3.4. qPCR assessment**

Figure (7) summarises gene expression for the composite model, including both HAOB and NHOK cell components. Of all genes evaluated, COL1 demonstrated the highest level of expression. Bone-specific genes such as ALP, OC, ON, and OP were detected, with ON expressed in high quantities. Genes encoding CK10 and CK13 were expressed, and were not significantly different.

**3.5. ELISA**

ELISA results for COL1, ON, and OC were consistent with the qPCR findings. COL1 demonstrated a significantly increased protein concentration in comparison to ON and OC. ON, in turn, was higher than OC (Figure 8).

**4. Discussion**

There is an increasingly recognized need to engineer tissue equivalents for both clinical and experimental applications. In this study, we have developed and characterized an *in vitro* 3D human alveolar osteomucosal construct that replicates the natural anatomical relationship of oral mucosal tissue and the underlying bone.

In 3D culture, cell viability is influenced by several factors including the scaffold and culture environment. Calcium phosphate and collagen constitute the main elements of the extracellular matrix of bone and oral mucosa, respectively.<sup>(17)</sup> Therefore, due to their biocompatibility, they have been widely used in tissue engineering as scaffolds to support cells growth without compromising their vitality.<sup>(18)</sup> The culture environment, on the other hand, that promotes mass transfer and nutrient delivery is another important factor to maintain cell vitality. In our study, growing OMM in a static culture raised no problem due to the hydrophilic, high water-containing networks of collagen hydrogel that enhance permeability for oxygen, nutrients and water-soluble metabolites.<sup>(19)</sup> Ceramic-based bone model, by contrast, required a dynamic flow to improve nutrient and waste diffusion because the static culture is only sufficient to nourish the thin superficial layer, approximately 100-200µm, contacting the medium.<sup>(20)</sup> As the cells increase in number, so does their metabolic demand and the build-up of waste products. Consequently, the deeper cells in the tissue interior can be deprived of oxygen and nutrients source in long-term static culture conditions. For this reason, the total culture time of the composite tissue after combining the hard and soft tissue constructs was limited to an additional 5 days at the static air/liquid interface in this study.

We have shown that the histological structure and expression of key markers of epithelial differentiation in OMM were comparable to those of its normal tissue counterpart. OMM displayed the characteristics of a para-keratinized epithelium, which suggests that the

keratinocytes used in this model retain the para-keratinized status of the original oral mucosa from which they were derived.<sup>(21)</sup>

The control of keratinocyte in proliferation and differentiation is multifactorial. Several studies have confirmed the role of fibroblasts in epithelial development through the stimulation of keratinocyte proliferation, migration, and keratin expression.<sup>(22, 23)</sup> Fibroblasts establish such growth-promoting roles through paracrine cross talk between NHOFs and NHOKs via cytokines such as heparin-binding EGF-like growth factor (HB-EGF), Interleukin 1 alpha (IL-1 $\alpha$ ) and Transforming growth factor beta 1 (TGF- $\beta$ 1).<sup>(24)</sup> This function requires an optimal fibroblast density, as the presence of either excessive or inadequate numbers of fibroblast will adversely affect epithelium morphogenesis, leading to differentiation markers being inappropriately expressed.<sup>(25)</sup> In our models, optimal fibroblast seeding density in order to support an anatomically representative epithelial layer was found to be  $2 \times 10^5$  cells per model. Keratinocyte senescence may also impact on the capacity to achieve anatomically representative epithelia in tissue culture models. Due to sustained telomerase expression within primary cells, sequential sub culturing may restrict the capacity of keratinocytes to divide once seeded into a 3D model, and therefore it is recommended that the use of keratinocytes in tissue substitute constructs is limited to passage 3 or less.<sup>(26)</sup>

The proper functionality of keratinocytes is important not only for epithelial layer formation, but also for epithelial-connective tissue attachment and cell-cell adhesion, which are essential for achieving an accurate, functional mucosal substitute. Our data, consistent with data from other studies, has confirmed that cells within the 3D models actively synthesised the ultrastructural components including desmosomes, hemidesmosomes, and basement membrane required for this structural stability.<sup>(27, 28)</sup>

Although collagen I is a non-specific marker of osteogenesis, relatively high levels were expressed in our model compared to other osteogenic genes; this may be due to a number of reasons. Firstly, this marker constitutes the most abundant component of bone extracellular matrix (90% of the organic component) and becomes upregulated during bone formation.<sup>(29)</sup> Secondly, ascorbic acid was added as a component of the culture medium in order to maintain the osteoblastic phenotype of bone-derived cells; ascorbic acid is known to stimulate of cell growth and collagen synthesis in osteoblasts.<sup>(30)</sup> The hydroxylation of proline residues of procollagen is increased to approximately 40% by ascorbate, which is known to stabilize the collagen triple helix.<sup>(31)</sup> Thirdly, although collagen I is the main organic component secreted by osteoblasts, it is also produced in abundance by fibroblasts<sup>(32, 33)</sup>, and therefore the fibroblastic component of the model may have contributed to the collagen levels observed.

We undertook analysis of further osteoblastic markers, including Osteocalcin, Osteopontin, Osteonectin and ALP. ALP, like Collagen I, is expressed in tissues other than bone and therefore its expression cannot be considered specific, although it is synthesised by osteoblasts and has been used to assess osteoblast phenotype and matrix mineralization.<sup>(34)</sup> Conversely, Osteocalcin, Osteopontin, and Osteonectin are major non-collagenous, bone-specific proteins that play profound roles in bone formation.<sup>(29)</sup> Osteonectin, in particular, is localized to mineralized bone trabeculae and is present at higher concentrations within extracellular matrix than in osteocytes. It selectively binds to collagen I and the resultant osteonectin-collagen complexes initiate mineral phase deposition by binding synthetic apatite crystals and free calcium ions.<sup>(35)</sup> Interestingly, Osteonectin can be demonstrated in active osteoblasts and osteoprogenitor cells as well as in young osteocytes, but not in aged, quiescent osteocytes; the protein is therefore a reliable marker of functional osteoblasts.<sup>(36)</sup> The simultaneous expression of Osteonectin and its encoding gene, SPARC, strongly

suggests that HOBs maintained their phenotypic characteristics in spite of a protracted culture period of 2 months.

The expression of all osteoblast-associated molecules varies over the different stages of bone development, and therefore the expression profiles observed in our models, which were cultured over a relatively short period compared to that of normal human bone turnover may vary somewhat to that observed *in vivo*. For example, ALP increases in the initial stages of bone formation, yet decreases as mineralization progresses, whereas osteopontin is first detected in young bone, whilst Osteocalcin appears towards the end of the mineralization process.<sup>(37)</sup>

5. Conclusion

This study demonstrates that tissue engineered tri-layered reconstructs based on primary human alveolar osteoblasts cultured in porous hydroxyapatite/tricalcium phosphate scaffolds adhered to collagen-embedded gingival fibroblasts overlain with primary gingival keratinocytes cultured at the air/liquid interface, were able to mimic the native alveolar bone and overlaying full-thickness mucosal structures. The engineered combined hard and soft tissue provides scope to act as a valuable alternative to 2D and animal models for various *in vitro* and potential *in vivo* applications. Further experiments are underway to assess the suitability of this 3D model for *in vitro* evaluation of bone invasion of oral cancer as well as development of *in vitro* tissue engineered models of osseointegrated dental implants using the 3D composite bone mucosal system.

Acknowledgement

The authors would like to thank Abdurahman El-Awa, Yusuf Alzayani, Ei Leen Lim, Claire Field, and all the other surgeons who provided us with bone chips and oral mucosa tissue. We acknowledge Kirsty Franklin for her help and support in the tissue culture laboratory, Chris Hill for his assistance with electron microscopy services, Rebecca Goodchild and Ceramisys LTD, UK for providing the bone scaffolds.

#### **Conflict of interests**

The authors declare that there is no conflict of interests regarding the publication of this paper.

References

1. Lanza, R.P., Langer, R.S., and Vacanti, J. Principles of tissue engineering. Fourth edition. ed: Amsterdam : Academic Press, 2014.

2. Rouwkema, J., Gibbs, S., Lutolf, M.P., Martin, I., Vunjak-Novakovic, G., and Malda, J. In vitro platforms for tissue engineering: implications for basic research and clinical translation. J Tissue Eng Regen Med **5**, e164, 2011.

3. Khoruzhenko, A.I. 2D- and 3D- cell culture. Biopolymers and Cell **27**, 17, 2011.

4. van der Worp, H.B., Howells, D.W., Sena, E.S., Porritt, M.J., Rewell, S., Collins, V., and Macleod, M.R. Can Animal Models of Disease Reliably Inform Human Studies? PLoS Medicine **7**, e1000245, 2010.

5. Pallua, N., and Suschek, C.V. Tissue engineering: from lab to clinic. London,Berlin: Springer; 2010.

6. Sun, J., Hou, X.-K., and Zheng, Y.-X. Restore a 9 mm diameter osteochondral defect with gene enhanced tissue engineering followed mosaicplasty in a goat model. Acta Orthopaedica et Traumatologica Turcica **50**, 464, 2016.

7. Ruan, S.Q., Yan, L., Deng, J., Huang, W.L., and Jiang, D.M. Preparation of a biphasic composite scaffold and its application in tissue engineering for femoral osteochondral defects in rabbits. International Orthopaedics, 1, 2017.

8. Park, C.H., Rios, H.F., Jin, Q., Sugai, J.V., Padial-Molina, M., Taut, A.D., Flanagan, C.L., Hollister, S.J., and Giannobile, W.V. Tissue engineering bone- ligament complexes using fiber- guiding scaffolds. Biomaterials 2011.

9. Almela, T., Brook, I., and Moharamzadeh, K. Development of three-dimensional tissue engineered bone-oral mucosal composite models. J Mater Sci: Mater Med 27:65, 2016.

10. Moharamzadeh, K., Brook, I., Noort, R., Scutt, A., Smith, K., and Thornhill, M. Development, optimization and characterization of a full-thickness tissue engineered human

- oral mucosal model for biological assessment of dental biomaterials. *J Mater Sci: Mater Med* **19**, 1793, 2008.
11. Rheinwald, J.G., and Green, H. Serial cultivation of strains of human epidermal keratinocytes: the formation of keratinizing colonies from single cells. *Cell* **6**, 331, 1975.
12. Mailhot, J.M., and Borke, J.L. An isolation and in vitro culturing method for human intraoral bone cells derived from dental implant preparation sites. *Clinical Oral Implants Research* **9**, 43, 1998.
13. Clausen, C., Hermund, N.U., Donatsky, O., and Nielsen, H. Characterization of human bone cells derived from the maxillary alveolar ridge. *Clinical Oral Implants Research* **17**, 533, 2006.
14. Dongari-Bagtzoglou, A., and Kashleva, H. Development of a highly reproducible three-dimensional organotypic model of the oral mucosa. *Nat Protoc* **1**, 2006.
15. Kriegebaum, U., Mildenerger, M., Mueller-Richter, U.D.A., Klammert, U., Kuebler, A.C., and Reuther, T. Tissue engineering of human oral mucosa on different scaffolds: in vitro experiments as a basis for clinical applications. *Oral Surgery, Oral Medicine, Oral Pathology and Oral Radiology* **114**, S190, 2012.
16. Morgan, P.R., Shirlaw, P.J., Johnson, N.W., Leigh, I.M., and Lane, E.B. Potential applications of anti-keratin antibodies in oral diagnosis. *Journal of oral pathology* **16**, 212, 1987.
17. Nanci, A. *Ten Cate oral histology : development, structure, and function*. 8th ed. / Antonio Nanci. ed. St. Louis, Mo.: St. Louis, Mo. : Elsevier, 2013.
18. Tayebi, L., and Moharamzadeh, K. *Biomaterials for oral and dental tissue engineering*: Oxford : Woodhead Publishing, 2017.



19. Peppas, N.A., Hilt, J.Z., Khademhosseini, A., and Langer, R. Hydrogels in Biology and Medicine: From Molecular Principles to Bionanotechnology. *Advanced Materials* **18**, 1345, 2006.
20. Rouwkema, J., Rivron, N.C., and van Blitterswijk, C.A. Vascularization in tissue engineering. *Trends Biotechnol* **26**, 434, 2008.
21. Chai, W.L., Moharamzadeh, K., Van Noort, R., Brook, I.M., Emanuelsson, L., and Palmquist, A. Development of a novel model for the investigation of implant- soft tissue interface. *Journal of Periodontology* **81**, 1187, 2010.
22. Okazaki, M., Yoshimura, K., Suzuki, Y., and Harii, K. Effects of subepithelial fibroblasts on epithelial differentiation in human skin and oral mucosa: heterotypically recombined organotypic culture model. *Plastic and reconstructive surgery* **112**, 784, 2003.
23. Rakhorst, H., Tra, W., Van Neck, J.W., Van Osch, G., Hovius, S., El Ghalbzouri, A., and Hofer, S.O.P. Fibroblasts Accelerate Culturing of Mucosal Substitutes. *Tissue Engineering* **12**, 2321, 2006.
24. Wang, Z., Wang, Y., Farhangfar, F., Zimmer, M., and Zhang, Y. Enhanced Keratinocyte Proliferation and Migration in Co- culture with Fibroblasts ( Keratinocyte Proliferation and Migration). *PLoS ONE* **7**, e40951, 2012.
25. El Ghalbzouri, A., Gibbs, S., Lamme, E., Van Blitterswijk, C.A., and Ponec, M. Effect of fibroblasts on epidermal regeneration. *British Journal of Dermatology* **147**, 230, 2002.
26. Ng, M.H., Aminuddin, B.S., Hamizah, S., Lynette, C., Mazlyzam, A.L., and Ruszymah, B.H.I. Correlation of donor age and telomerase activity with in vitro cell growth and replicative potential for dermal fibroblasts and keratinocytes. *Journal of Tissue Viability* **18**, 109, 2009.

27. Tra, W.M.W., Van Neck, J.W., Hovius, S.E.R., Perez-Amodio, S., and Van Osch, G.J.V.M. Characterization of a three- dimensional mucosal equivalent: Similarities and differences with native oral mucosa. *Cells Tissues Organs* **195**, 185, 2012.
28. Chai, W.L., Van Noort, R., Moharamzadeh, K., Brook, I.M., Emanuelsson, L., and Palmquist, A. Ultrastructural analysis of implant- soft tissue interface on a three dimensional tissue- engineered oral mucosal model. *Journal of Biomedical Materials Research - Part A* **100**, 269, 2012.
29. Allori, A., Sillon, A., and Warren, S. Biological Basis of Bone Formation, Remodeling, and Repair-- Part I: Biochemical Signaling Molecules. *Tissue Engineering*, **14**, 259, 2008.
30. Choi, K.-M., Seo, Y.-K., Yoon, H.-H., Song, K.-Y., Kwon, S.-Y., Lee, H.-S., and Park, J.-K. Effect of ascorbic acid on bone marrow- derived mesenchymal stem cell proliferation and differentiation. *Journal of Bioscience and Bioengineering* **105**, 586, 2008.
31. Berg, R.A., and Prockop, D.J. The thermal transition of a non- hydroxylated form of collagen. Evidence for a role for hydroxyproline in stabilizing the triple- helix of collagen. *Biochemical and Biophysical Research Communications* **52**, 115, 1973.
32. Kishimoto, Y., Saito, N., Kurita, K., Shimokado, K., Maruyama, N., and Ishigami, A. Ascorbic acid enhances the expression of type 1 and type 4 collagen and SVCT2 in cultured human skin fibroblasts. *Biochemical and Biophysical Research Communications* **430**, 579, 2013.
33. Schwarz, R.I. Collagen I and the fibroblast: High protein expression requires a new paradigm of post- transcriptional, feedback regulation. *Biochemistry and Biophysics Reports* **3**, 38, 2015.
34. Masrour Roudsari, J., and Mahjoub, S. Quantification and comparison of bone- specific alkaline phosphatase with two methods in normal and paget's specimens. *Caspian journal of internal medicine* **3**, 478, 2012.

35. Termine, J.D., Kleinman, H.K., Whitson, S.W., Conn, K.M., McGarvey, M.L., and Martin, G.R. Osteonectin, a bone- specific protein linking mineral to collagen. *Cell* **26**, 99, 1981.

36. Jundt, G., Berghäuser, K., Termine, J., and Schulz, A. Osteonectin — a differentiation marker of bone cells. *Cell and Tissue Research* **248**, 409, 1987.

37. Kim, M.-C., Hong, M.-H., Lee, B.-H., Choi, H.-J., Ko, Y.-M., and Lee, Y.-K. Bone Tissue Engineering by Using Calcium Phosphate Glass Scaffolds and the Avidin– Biotin Binding System. *The Journal of the Biomedical Engineering Society* **43**, 3004, 2015.

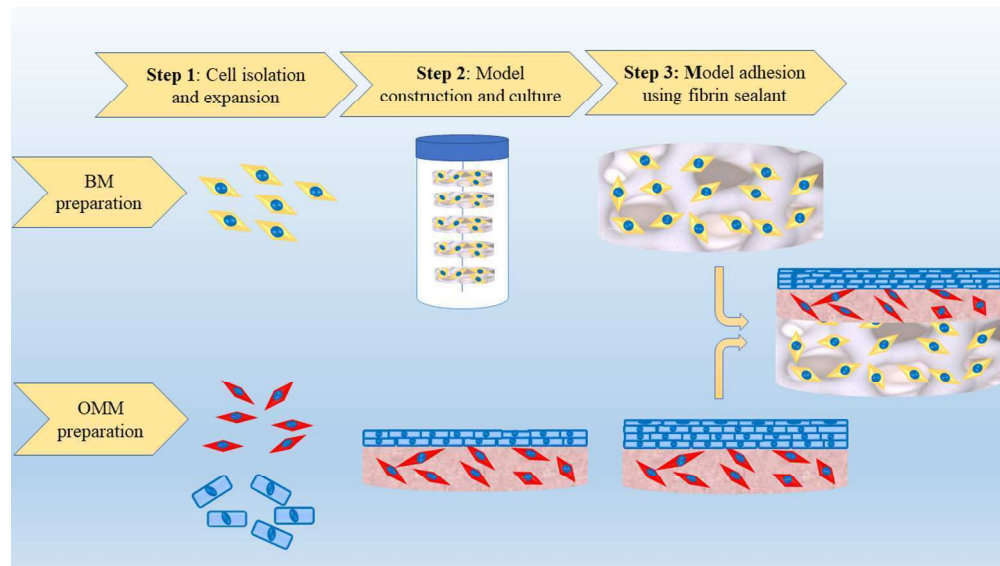


Figure 1. Schematic illustration of the preparation of OMM, BM, and ABMM. The procedure involved 3 main steps. First; HAObS, NHOFS, and NHOKs were isolated from oral tissues and cultivated in monolayer culture. Second; BMs were prepared by seeding HAObS in HA/TCP scaffold and cultured in spinner bioreactor while OMMs were prepared from fibroblast-populated collagen gel and air liquid interface culture oral keratinocytes. Third; Combination of BM and OMM using adhesive fibrin to form ABMM.

338x190mm (300 x 300 DPI)

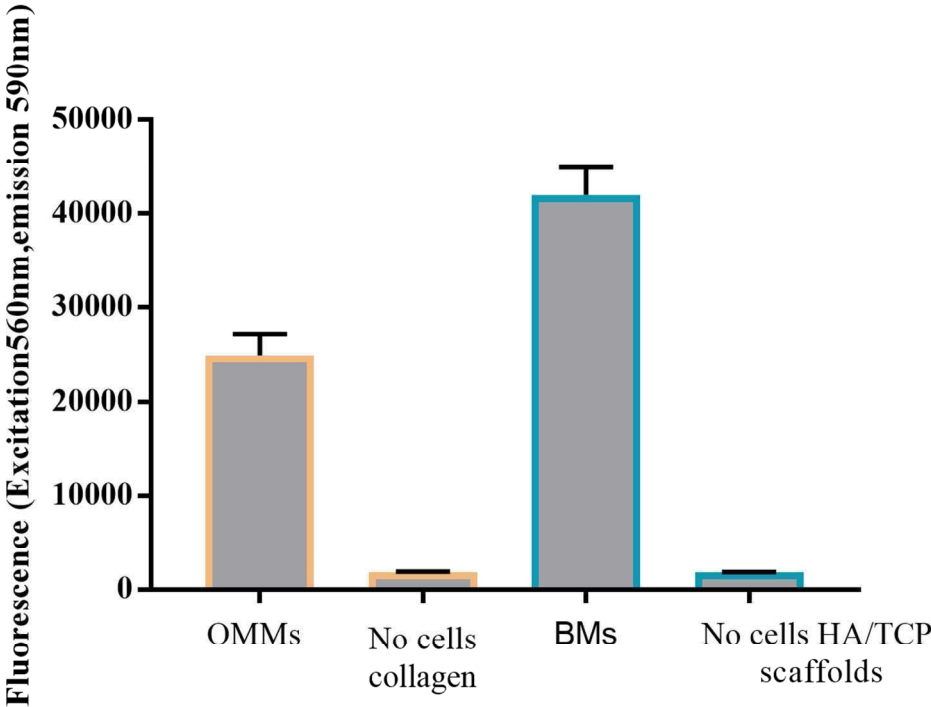


Figure 2. Vitality assessment of OMMs and BMs. The figure shows the activity of HAOBs within HA/TCP scaffold as well as NHOFs and NHOKs in OMMs after 17 days of culture.

107x83mm (300 x 300 DPI)

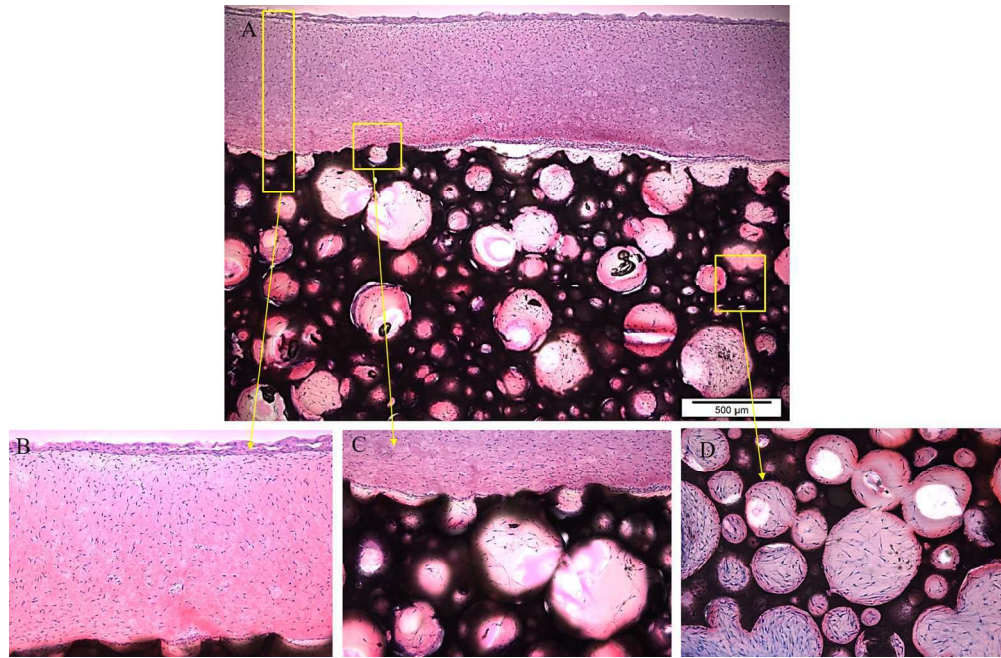


Figure 3. H&E-stained histological sections of ABMM showing (A) full-thickness multi-layered bone and mucosa; and magnified images of (B) oral mucosa part; (C) bone-mucosal interface; and (D) bony part showing the pores of the scaffold filled with osteoblasts and extracellular matrix (Original magnification A  $\times$  4; B, C, and D  $\times$  10).

143x93mm (300 x 300 DPI)



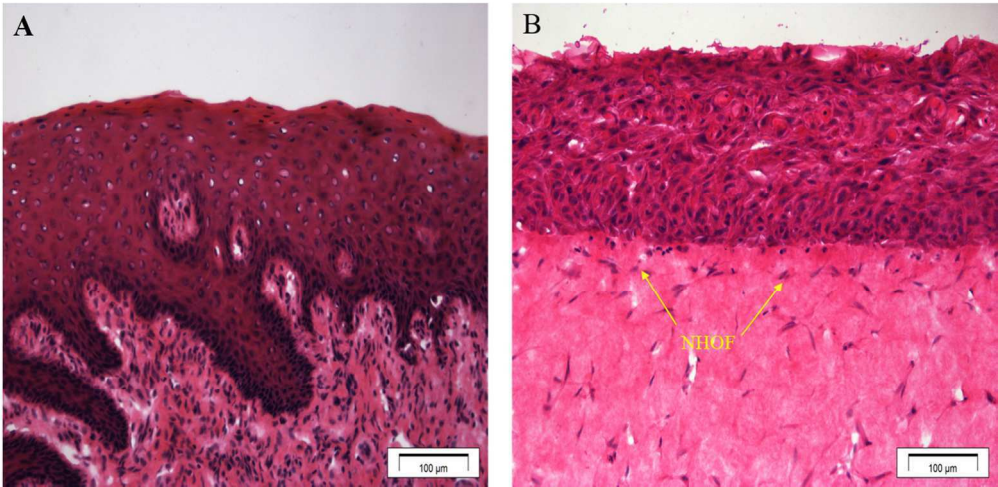


Figure 4. H&E-stained histological sections of (A) NOM; and (B) OMM showing a well-differentiated stratified squamous epithelial layer with viable fibroblasts scattered in the connective tissue layer (Original magnification  $\times 20$ ).

123x60mm (300 x 300 DPI)

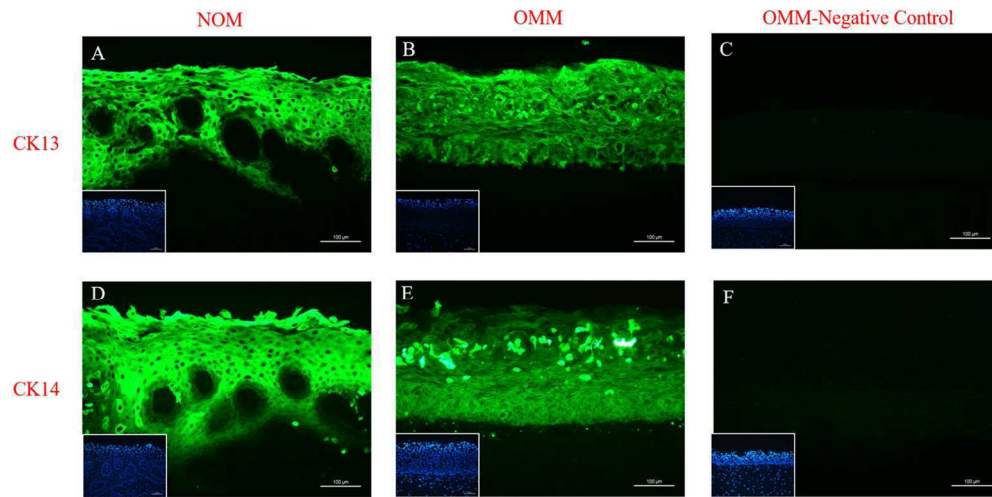


Figure 5. Immunofluorescent staining of the oral mucosa showing (A and D) both epithelial markers CK13 and CK14 were well detected in the NOM; (B and E) strong expression of CK13 and CK14 in the OMM; and (C, F) negative control (Original magnification  $\times 20$ ; the lower left boxes are DAPI stain).

127x63mm (300 x 300 DPI)



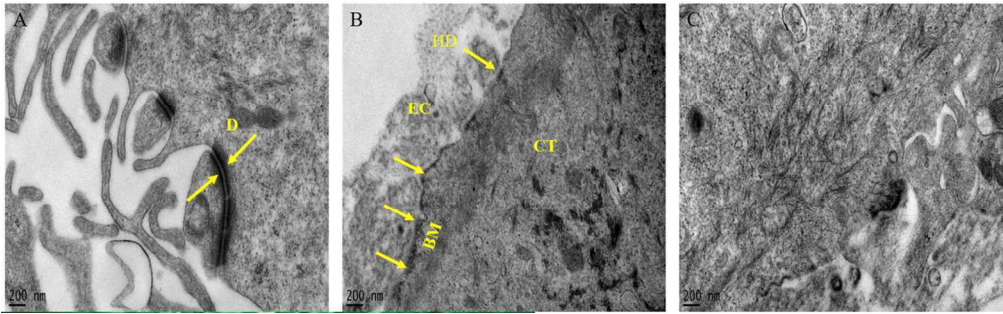


Figure 6. Ultrastructural analysis of the OMM by transmission electron microscopy showing (A) numerous desmosomes (D) between adjacent epithelial cells; (B) basement membrane (BM) formed all along the interface between the epithelial cell (EC) and connective tissue (CT) with the presence of hemidesmosomes (HD); and (C) newly synthesized collagen I fibrils in the connective tissue (Original magnification  $\times 50000$ ).

127x39mm (300 x 300 DPI)

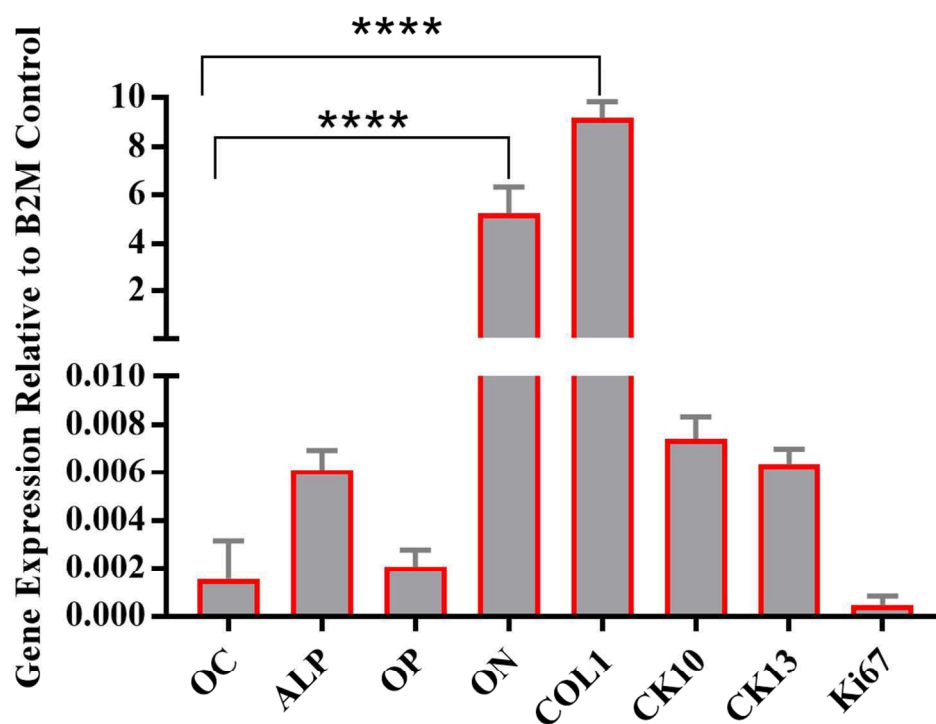


Figure 7. The gene expression of HAOBs and NHOKs in the ABMM as evaluated with PCR analysis. The osteogenic markers; OC, ALP, OP, ON, and COL1, in addition to the epithelial markers; CK10, CK13 were detected. Statistical significance was determined as  $p < 0.05$  from control (\*\*\*\*  $P < 0.0001$ ).

97x78mm (300 x 300 DPI)

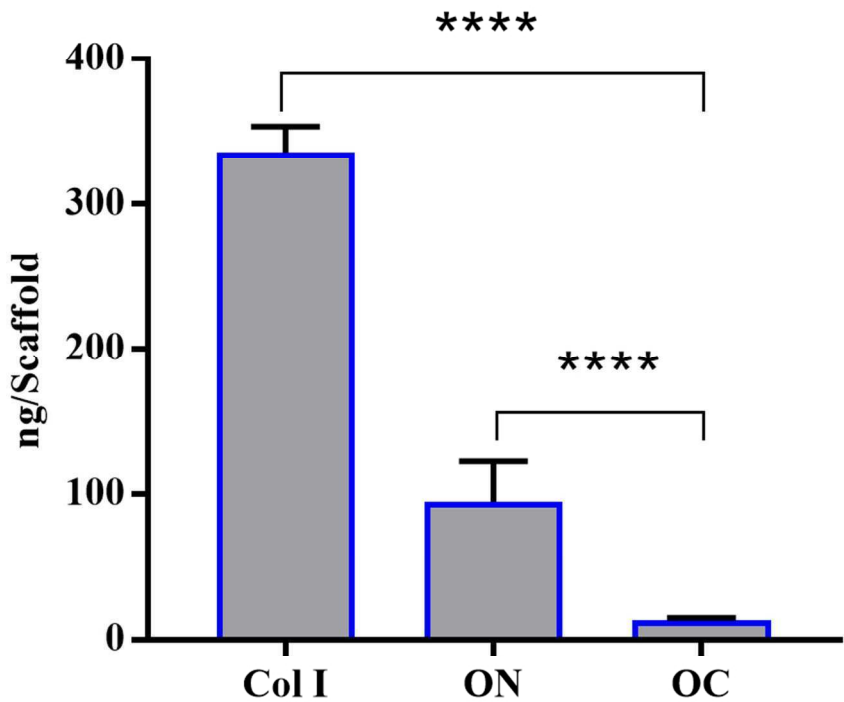


Figure 8. Protein expression of Collagen I, Osteonectin, and Osteocalcin in ABMM analyzed by ELISA. Statistical significance was determined as  $p < 0.05$  (\*\*\*\*  $P < 0.0001$ ).

87x69mm (300 x 300 DPI)

**Figure legends:**

**Figure 1. Schematic illustration of the preparation of OMM, BM, and ABMM.** The procedure involved 3 main steps. First; HAOBs, NHOFs, and NHOKs were isolated from oral tissues and cultivated in monolayer culture. Second; BMs were prepared by seeding HAOBs in HA/TCP scaffold and cultured in spinner bioreactor while OMMs were prepared from fibroblast-populated collagen gel and air liquid interface culture oral keratinocytes. Third; Combination of BM and OMM using adhesive fibrin to form ABMM.

**Figure 2. Vitality assessment of OMMs and BMs.** The figure shows the activity of HAOBs within HA/TCP scaffold as well as NHOFs and NHOKs in OMMs after 17 days of culture.

**Figure 3. H&E-stained histological sections of ABMM** showing (A) full-thickness multi-layered bone and mucosa; and magnified images of (B) oral mucosa part; (C) bone-mucosal interface; and (D) bony part showing the pores of the scaffold filled with osteoblasts and extracellular matrix (Original magnification A  $\times$  4; B, C, and D  $\times$  10).

**Figure 4. H&E-stained histological sections of (A) NOM; and (B) OMM** showing a well-differentiated stratified squamous epithelial layer with viable fibroblasts scattered in the connective tissue layer (Original magnification  $\times$  20).

**Figure 5. Immunofluorescent staining of the oral mucosa** showing (A and D) both epithelial markers CK13 and CK14 were well detected in the NOM; (B and E) strong expression of CK13 and CK14 in the OMM; and (C, F) negative control (Original magnification  $\times$  20; the lower left boxes are DAPI stain).

**Figure 6. Ultrastructural analysis of the OMM by transmission electron microscopy** showing (A) numerous desmosomes (D) between adjacent epithelial cells; (B) basement membrane (BM) formed all along the interface between the epithelial cell (EC) and

connective tissue (CT) with the presence of hemidesmosomes (HD); and (C) newly synthesized collagen I fibrils in the connective tissue (Original magnification  $\times 50000$ ).

**Figure 7. The gene expression of HAOBs and NHOKs in the ABMM as evaluated with PCR analysis.** The osteogenic markers; OC, ALP, OP, ON, and COL1, in addition to the epithelial markers; CK10, CK13 were detected. Statistical significance was determined as  $p<0.05$  from control (\*\*\*\*  $P<0.0001$ ).

**Figure 8.** Protein expression of Collagen I, Osteonectin, and Osteocalcin in ABMM analyzed by ELISA. Statistical significance was determined as  $p<0.05$  (\*\*\*\*  $P<0.0001$ ).